

Magnetism and giant magnetoresistance of $\text{YMn}_6\text{Sn}_{6-x}\text{Ga}_x$ ($x=0-1.8$) compounds

Shao-ying Zhang, Peng Zhao, Zhao-hua Cheng, Run-wei Li, Ji-rong Sun, Hong-wei Zhang, and Bao-gen Shen
*State Key Laboratory of Magnetism, Institute of Physics and Center for Condensed Matter Physics, Chinese Academy of Sciences,
 P. O. Box 603, Beijing 100080, People's Republic of China*

(Received 15 November 2000; revised manuscript received 12 April 2001; published 8 November 2001)

Magnetic and transport properties of $\text{YMn}_6\text{Sn}_{6-x}\text{Ga}_x$ ($0 \leq x \leq 1.8$) compounds with the HfFe_6Ge_6 -type structure were investigated. It was found that Ga substitution leads to a contraction of the unit-cell volume. A transition from an antiferromagnetic to a ferromagnetic (or ferrimagnetic) state can be observed for $0.1 \leq x \leq 0.2$ with increasing temperature. The antiferro-ferromagnetic transition for samples with $x \leq 0.2$ can also be induced by an external field. The metamagnetic transition field is very low, and decreases with increasing Ga concentration. Higher Ga concentration ($x > 0.2$) leads to the samples being ferromagnetic in the whole temperature range below the Curie temperature. Ga substitution weakens the interlayer magnetic coupling between the Mn spins. Corresponding to the metamagnetic transition, a magnetoresistance as large as 32% in a field of 5 T was observed at 5 K for the sample with $x=0.2$. Results from the ^{119}Sn Mössbauer spectra indicate that the Mn-Mn coupling through the "Mn-Sn-Sn-Mn" slab change from antiferromagnetic in YMn_6Sn_6 to ferromagnetic by the substitution of Ga for Sn.

DOI: 10.1103/PhysRevB.64.212404

PACS number(s): 75.30.-m

Rare-earth compounds of the RMn_6X_6 and RMn_2X_2 (R = rare-earth elements and $X = \text{Sn}$ or Ge) types have been reported to possess various magnetic structures and interesting magnetic properties.¹⁻⁴ All these compounds are composed of R and Mn layers alternately stacked along the c axis. Up to now, the magnetic structures and magnetic properties of the ternary RMn_6X_6 compounds have been widely investigated. It has been found that the magnetic structures and magnetic properties are very sensitive to the Mn-Mn distances as well as to the nature of the R element. Among them, the YMn_6Sn_6 compound is antiferromagnetic over the whole temperature range below Néel temperature $T_N = 333$ K. The magnetic structures are characterized by ferromagnetic (001) Mn planes. The interplane Mn moments through the Mn-Sn-Sn-Mn slab are always parallel, while those occurring through the Mn-(Sn-R)-Mn slab rotate with a nonconstant angle.^{1,5} Such a helical magnetic structure suggests that the magnetic interactions within the involved slab are very sensitive to the nature of the R element and even slight modifications of the chemical bond.

In RMn_2Ge_2 and RMn_6X_6 compounds, including YMn_6Sn_6 , a metamagnetic transition is observed from an antiferromagnetic state toward a ferromagnetic state, which can be induced by an applied field.⁶⁻⁸ The transition between the two different magnetic states takes place at a critical field, and is of first-order. The mechanism leading to the metamagnetic transition was found to be extremely sensitive to the Mn-Mn distance. In addition, in many systems with metamagnetic transitions, giant magnetoresistance (GMR) has been observed.⁹⁻¹² Though many models have been proposed to explain GMR, it is presently accepted that GMR is caused by spin-dependent electron scattering when the magnetic structure of the sample changes. So the magnetoresistance data can provide an evidence of the magnetic transition.

In this paper, we report the effects of Ga substitution for Sn on the magnetic and transport properties of the $\text{YMn}_6\text{Sn}_{6-x}\text{Ga}_x$ ($0 \leq x \leq 1.8$) series. As Y is nonmagnetic,

these compounds offer the possibility for a study of the Mn-Mn interactions in relation to the Mn-Mn interatomic distance, temperature, and magnetic field. Unlike substitution for Mn, substitution for Sn by Ga does not involve dilution of the magnetic Mn sublattice and thus the effect of the Mn-Mn interatomic distance on the antiferromagnetic ordering can be better studied without the effect of the Mn dilution.

$\text{YMn}_6\text{Sn}_{6-x}\text{Ga}_x$ ($0 \leq x \leq 1$) polycrystalline samples were synthesized by melting the constituent elements in a high-purified Ar atmosphere by the standard arc-furnace technique. The purity of the elements was better than 99.9%. An excess of Y, Mn, and Ga over the stoichiometric amount was added to compensate for the mass loss during melting. All samples were annealed at 1023 K for 10 days and rapidly cooled down to room temperature. X-ray diffraction studies were carried out using a Rigaku Rint 1400 diffractometer with CuK_α radiation at room temperature. All samples display peaks characteristic for the HfFe_6Ge_6 -type structure with minor Mn_3Sn_2 as impurity phase. The lattice constants of all compounds are listed in Table I. Substitution of Ga for Sn leads to a decrease of the lattice constants a and c due to

TABLE I. The lattice constants $a, c, c/a$ and unit cell volume v of $\text{YMn}_6\text{Sn}_{6-x}\text{Ga}_x$ compounds.

Compounds	a (nm)	c (nm)	c/a	v (nm ³)
YMn_6Sn_6	0.5536	0.9024	1.630	0.2395
$\text{YMn}_6\text{Sn}_{5.9}\text{Ga}_{0.1}$	0.5528	0.9013	1.630	0.2386
$\text{YMn}_6\text{Sn}_{5.8}\text{Ga}_{0.2}$	0.5524	0.9002	1.630	0.2379
$\text{YMn}_6\text{Sn}_{5.7}\text{Ga}_{0.3}$	0.5517	0.8991	1.630	0.2370
$\text{YMn}_6\text{Sn}_{5.4}\text{Ga}_{0.6}$	0.5506	0.8972	1.629	0.2356
$\text{YMn}_6\text{Sn}_{5.1}\text{Ga}_{0.9}$	0.5491	0.8946	1.629	0.2336
$\text{YMn}_6\text{Sn}_{4.8}\text{Ga}_{1.2}$	0.5485	0.8939	1.630	0.2329
$\text{YMn}_6\text{Sn}_{4.5}\text{Ga}_{1.5}$	0.5468	0.8913	1.630	0.2308
$\text{YMn}_6\text{Sn}_{4.2}\text{Ga}_{1.8}$	0.5457	0.8890	1.629	0.2293

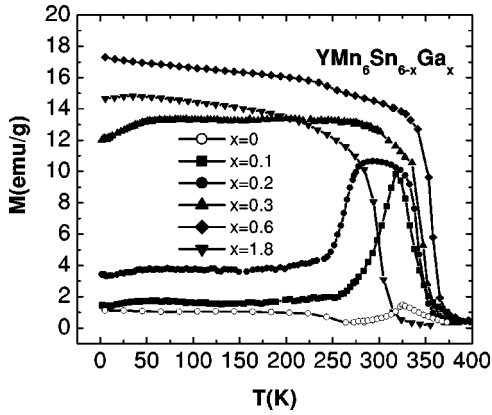


FIG. 1. Temperature dependence of the magnetization of $\text{YMn}_6\text{Sn}_{6-x}\text{Ga}_x$ compounds at a magnetic field of 0.5 kOe.

the smaller ionic radius of Ga compared with Sn. The ratio of c/a is a constant for all samples, indicating an isotropic contraction. The Mn–Mn interatomic distance in (001) Mn planes is equal to the lattice constant $a/2$. The Mn–Mn interatomic distance between interplanes is proportional to the lattice constant c . So the decrease of the lattice constants by substitution of Ga for Sn means the reduction of the interatomic distances of Mn atoms, both within and between the layers.

The magnetization measurements on free-powder samples were carried out in the temperature range of 5–400 K using a superconducting quantum interference device (SQUID) magnetometer with a maximum field of 50 kOe. The temperature dependence of the magnetization M of $\text{YMn}_6\text{Sn}_{6-x}\text{Ga}_x$ compounds measured at a constant applied field of 0.5 kOe after zero field-cooling is shown in Fig. 1. Three concentration regions with different magnetic properties appear: (1) for $x=0$, the sample has antiferromagnetic properties; (2) for $0.1 \leq x \leq 0.2$, the samples undergo a magnetic transition from the antiferromagnetic to the ferromagnetic (or ferrimagnetic) state as the temperature rises; (3) for $x \geq 0.3$, the samples are ferromagnets in the whole temperature range below Curie temperature T_C . In the ferromagnetic region, the values of T_C increase first, reach the maximum of 367 K at $x=0.6$, and then decrease for larger x . The magnetic data are listed in Table II. The small step in the M - T

TABLE II. Magnetic data for $\text{YMn}_6\text{Sn}_{6-x}\text{Ga}_x$ compounds.

Compounds	Type of magnetic ordering	$T_{C,N}$ (K)	$\mu_{\text{Mn}}(\mu_B)$ (293 K)
YMn_6Sn_6	AF	327	
$\text{YMn}_6\text{Sn}_{5.9}\text{Ga}_{0.1}$	AF-F	318	1.12
$\text{YMn}_6\text{Sn}_{5.8}\text{Ga}_{0.2}$	AF-F	354	1.11
$\text{YMn}_6\text{Sn}_{5.7}\text{Ga}_{0.3}$	F	357	1.12
$\text{YMn}_6\text{Sn}_{5.4}\text{Ga}_{0.6}$	F	367	1.17
$\text{YMn}_6\text{Sn}_{5.1}\text{Ga}_{0.9}$	F	354	1.15
$\text{YMn}_6\text{Sn}_{4.8}\text{Ga}_{1.2}$	F	340	1.13
$\text{YMn}_6\text{Sn}_{4.5}\text{Ga}_{1.5}$	F	330	1.03
$\text{YMn}_6\text{Sn}_{4.2}\text{Ga}_{1.8}$	F	311	0.50

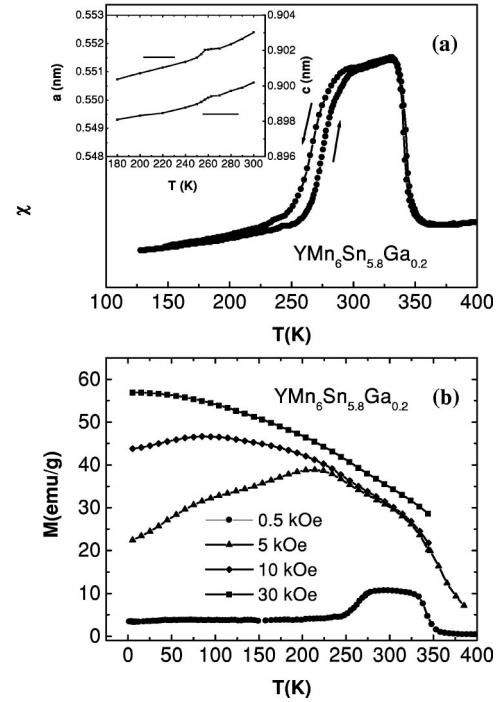


FIG. 2. Temperature dependence of the ac magnetic susceptibility (a) and the magnetization at different magnetic fields (b) for $\text{YMn}_6\text{Sn}_{5.8}\text{Ga}_{0.2}$. The inset of (a) shows the temperature dependence of the parameters a and c for $x=0.2$.

curves near 270 K may be a contribution from the impurity Mn_3Sn_2 [which orders ferromagnetically near 270 K (Ref. 1).]

To better understand the magnetic behavior of the sample with $x=0.2$, the temperature dependence of the ac magnetic susceptibility was measured with increasing and then with decreasing temperature. From Fig. 2(a), it is clear that the antiferro–ferromagnetic transition is a first-order due to a large temperature hysteresis observed. To prove that the antiferro–ferromagnetic transition is of first-order transition, the lattice constants a and c for $x=0.2$ were measured near the transition temperature range [shown in Fig. 2(a), inset]. Distinct anomalies of the lattice constants a and c near 257 K were observed, which can be taken as conclusive evidence supporting the first-order nature of the antiferro–ferromagnetic transition. We also measured the temperature dependence of the magnetization for the sample with $x=0.2$ at different magnetic fields. These results are shown in Fig. 2(b). In the low-temperature range, the magnetic properties of the antiferromagnetic phase show dependence on the external field. A higher external magnetic field can transform the sample into the ferromagnetic state. Similar phenomena were also reported in Refs. 1 and 13.

Figure 3(a) shows isothermal magnetization curves as a function of applied field at 293 K. For the samples with $x \geq 0.1$, the magnetization increases relatively faster at low fields and approaches saturation at high fields, indicating their ferromagnetic character. The saturation moment of the Mn atoms has been derived by extrapolating the M - H curve to $H=0$, and is presented in Table II. The Mn moment is 1.03 – $1.17\mu_B$ for samples with $0.1 \leq x \leq 1.5$, and then de-

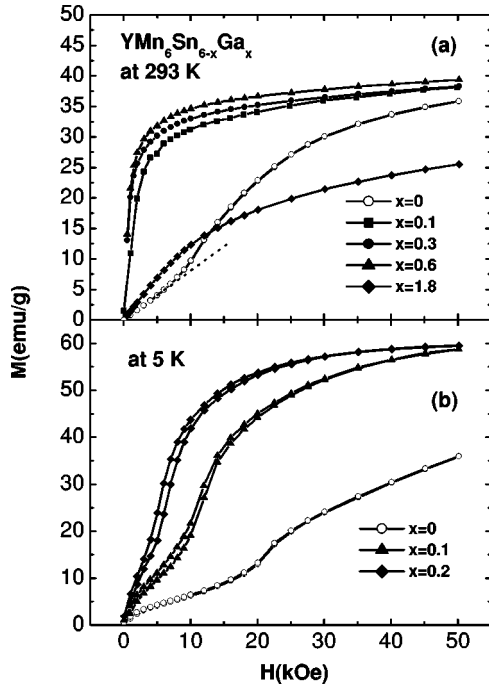


FIG. 3. Magnetization of $\text{YMn}_6\text{Sn}_{6-x}\text{Ga}_x$ as a function of applied magnetic field at 293 K (a) and 5 K (b).

increases strongly at higher x , consistent with the rapid decrease of T_C . These values of the Mn moment at room temperature are slightly lower than the result (about $1.25\mu_B$) reported for YMn_6Sn_6 ,⁵ which might arise from variations in the Mn $3d$ -band overlap due to the decrease of the Mn–Sn interatomic distance.

YMn_6Sn_6 is a pure antiferromagnet and preliminary neutron-diffraction experiments have given evidence for a helical arrangement of the Mn moments in this compound. The steep linear increase of the magnetization below 10 kOe shown in Fig. 3(a) can be interpreted as a rotation of the magnetization vectors of the Mn sublattices towards the direction parallel to the applied field. It is noteworthy that the magnetization deviates upward from the dotted straight line above 10 kOe. This abrupt increase at a critical magnetic field H_m indicates a metamagnetic transition from an antiferromagnetic to a ferromagnetic state. In order to clarify this metamagnetic transition, the M - H curves for samples with $x \leq 0.2$ were measured at 5 K in applied fields up to 50 kOe and then down to zero [see Fig. 3(b)]. The transition to the ferromagnetic state is seen to be accompanied by a clear hysteresis. It is likely therefore that the transition is of first-order, similar to that in GdMn_6Ge_6 .⁸ Even at 5 K, the metamagnetic transition field is still very low, and decreases with increasing Ga concentration for $x \leq 0.2$. The samples with $x > 0.2$ exhibit ferromagnetic behavior without any trace of metamagnetism. For simplicity, we consider three types of Mn–Mn interactions, a direct ferromagnetic interaction within the (001) Mn planes and two indirect interlayer interactions through the Mn–Sn–Sn–Mn and Mn–(R,Sn)–Mn slabs,¹⁴ at least one of which is antiferromagnetic. Due to the helical arrangement of the Mn moments, the data presented in Fig. 3(b) cannot be analyzed in terms of the two- or three-

sublattice models used for a collinear magnetic structure. However, the fact that the antiferro–ferromagnetic transition is easily achieved by changing the external magnetic field or chemical composition in $\text{YMn}_6\text{Sn}_{6-x}\text{Ga}_x$ suggests rather weak interlayer interactions, the ferromagnetic intralayer interaction remaining preponderant. The metamagnetic transition field decreases with increasing Ga concentration, demonstrating a weakening of the interlayer antiferromagnetic interaction. The decrease of the Mn–Mn interatomic distance, especially the Mn–Mn distance along the c axis, is one reason for this change of the magnetic interaction. The interlayer interactions through the Mn–Sn–Sn–Mn slab and the Mn–(R,Sn)–Mn slab are mediated by indirect superexchange via the conduction electrons, like the Ruderman–Kittel–Kasuya–Yosida (RKKY) interaction. Such an effect might be related to a change within the Mn–Sn bond. Another reason is the electronic structure. The investigation of the effect of electronic configuration is in progress.

¹¹⁹Sn Mössbauer spectra were recorded at room temperature without magnetic field. There are three Sn sites with the same number of Mn neighbors in the HfFe_6Ge_6 -type structure, i.e., Sn_1 ($2d$), Sn_2 ($2c$), and Sn_3 ($2e$). The hyperfine field at each Sn site should be proportional to the moment and the arrangement of nearby Mn atoms. It was found that the hyperfine field in YMn_6Sn_6 is 114 kOe at the Sn_1 site, 114 kOe at the Sn_2 site, and 175 kOe at the Sn_3 site. The hyperfine field changes to 121 kOe at the Sn_1 site, 181 kOe at the Sn_2 site, and 200 kOe at the Sn_3 site for the sample with $x = 0.6$. This means that the orientation of the Mn moment between the adjacent Mn layers through the Sn_2 site changes from nearly anti-parallel to almost parallel. In other words, the Mn–Mn coupling through the “Mn–Sn–Sn–Mn” slab change from antiferromagnetic for YMn_6Sn_6 to ferromagnetic by substitution of Ga for Sn. The coupling through the Mn–(R,Sn)–Mn slab is still unchanged (antiferromagnetic ordering). This gives support to the magnetic transition observed by magnetic measurements. A detailed study of the Mössbauer spectra of $\text{YMn}_6\text{Sn}_{6-x}\text{Ga}_x$ will be published elsewhere.¹⁵ A disagreement was reported in Ref. 5, that the Mn–Mn coupling through the “Mn–Sn–Sn–Mn” slab in YMn_6Sn_6 are systematically ferromagnetic. Further study of this aspect is required.

Magnetoresistance (MR) measurements were carried out using the standard four-probe dc technique with an electric current (100 mA) parallel to the magnetic field. The sample used in the MR measurements was a square cross-section rod of dimension $10 \times 2 \times 2$ mm³. Figure 4(a) shows the magnetic field dependence of the MR for the samples with $x \leq 0.2$ at 5 K. The ratio $[\rho(H) - \rho(0)] \times 100 / \rho(0)$ has been used to represent the MR. The magnitude of the MR for all the three samples is very small at low magnetic fields. The sudden development of negative MR around the critical field indicates that the compounds undergo a metamagnetic transition from an antiferromagnetic to a ferromagnetic state. Similar transitions in MR have earlier been observed in $\text{Ce}(\text{Fe}, \text{Al})_2$,¹⁶ $\text{Ce}(\text{Fe}, \text{Ru})_2$,¹² and SmMn_2Ge_2 (Ref. 17) compounds. The critical field, at which negative MR develops, decreases with increasing Ga content, coinciding closely with the metamagnetic transition field H_m observed in the

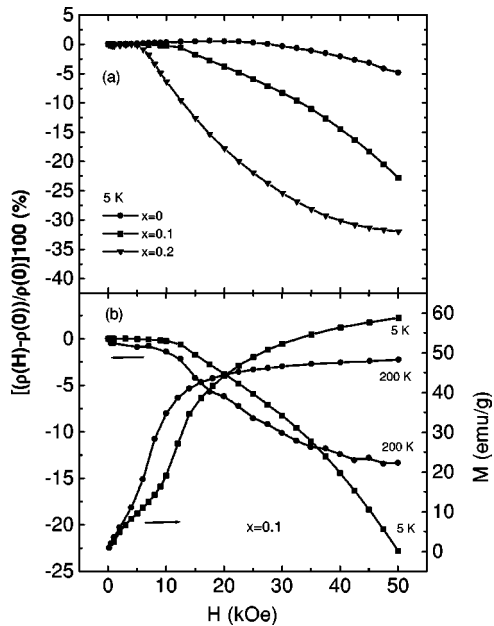


FIG. 4. Magnetic field dependence of the magnetoresistance MR of $\text{YMn}_6\text{Sn}_{6-x}\text{Ga}_x$ ($x \leq 0.2$) at 5 K (a) and MR and magnetization for sample with $x=0.1$ at 5 K and 200 K (b).

magnetization curves shown in Fig. 3(b). Figure 4(b) compares the magnetic-field dependence of MR and the magnetization for the sample with $x=0.1$ at 5 K and 200 K. It can be seen more clearly that the MR starts to increase when the metamagnetic transition occurs. Above the metamagnetic transition, the MR does not saturate up to the maximum applied field of 50 kOe. This indicates that the sample does not acquire a collinear ferromagnetic state but rather goes into a canted ferromagnetic state in the range of fields studied. An MR as large as 32% in a magnetic field of 50 kOe is gained at 5 K in the sample with $x=0.2$. The MR of the sample with $x=0.3$ without the metamagnetic transition is very small ($\leq 5\%$).

It is well recognized that the GMR in granular alloys and manganese oxides appear when spin moments, which are

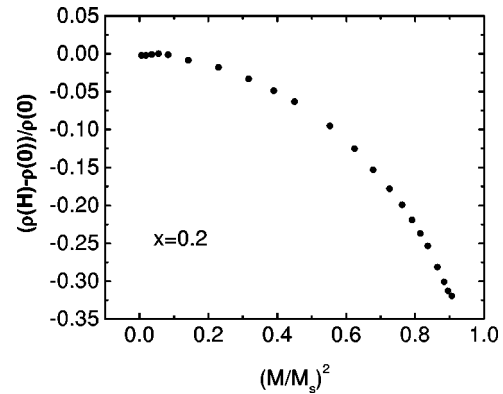


FIG. 5. Magnetoresistance $[\rho(H)-\rho(0)]/\rho(0)$ as a function of $(M/M_s)^2$ for sample with $x=0.2$.

randomly oriented in the materials, are aligned by an applied magnetic field. In this case, the behavior can be described by a formula $[\rho(H)-\rho(0)]/\rho(0) = A(M/M_s)^2$, where A is a coefficient which determines the magnitude of the MR and M_s is the saturation magnetization. If the MR observed in $\text{YMn}_6\text{Sn}_{6-x}\text{Ga}_x$ ($x \leq 0.2$) compounds is caused by the granular-type mechanism, the behavior of the MR might be scaled by the above formula. The $(M/M_s)^2$ dependence of $[\rho(H)-\rho(0)]/\rho(0)$ for $x=0.2$ is shown in Fig. 5. After the start of the metamagnetic transition, the MR cannot be scaled by the formula. Therefore, the appearance of MR in $\text{YMn}_6\text{Sn}_{6-x}\text{Ga}_x$ ($x \leq 0.2$) cannot be attributed to a granular mechanism. It is considered that the behavior of the MR found in $\text{YMn}_6\text{Sn}_{6-x}\text{Ga}_x$ ($x \leq 0.2$) compounds might result from the spin-flip scattering related to the metamagnetic transition from the antiferromagnetic to the ferromagnetic spin configuration.

This work was supported by the State Key Project of Fundamental Research and National Natural Sciences Foundation of China.

- ¹G. Venturini, B. Chafik El Idrissi, and B. Malaman, *J. Magn. Mater.* **94**, 35 (1991).
- ²G. Venturini, R. Welter, and B. Malaman, *J. Alloys Compd.* **185**, 99 (1992).
- ³K.S.V.L. Narashimhan *et al.*, *J. Appl. Phys.* **46**, 4957 (1975).
- ⁴A. Szytula and I. Szott, *Solid State Commun.* **40**, 199 (1981).
- ⁵G. Venturini, D. Fruchart, and B. Malaman, *J. Alloys Compd.* **236**, 102 (1996).
- ⁶A. Szytula, *Ferromagnetic Materials 5*, edited by K.H.J. Buschow (North-Holland, Amsterdam, 1991).
- ⁷F.M. Mulder *et al.*, *J. Alloys Compd.* **190**, L29 (1993).
- ⁸J.H.V.J. Brabers *et al.*, *J. Alloys Compd.* **198**, 127 (1993).
- ⁹M.N. Baibich *et al.*, *Phys. Rev. Lett.* **61**, 2472 (1988).
- ¹⁰J.Q. Xiao, J.S. Jiang, and C.L. Chien, *Phys. Rev. Lett.* **68**,

3749 (1992).

- ¹¹H. Samata, N. Sekiguchi, A. Sawabe, Y. Nagata, T. Uchiba, and M.D. Lan, *J. Phys. Chem. Solids* **59**, 377 (1998).
- ¹²H.P. Kunkel, X.Z. Zhou, P.A. Stampe, J.A. Cowen, and Gwyn Williams, *Phys. Rev. B* **53**, 15 099 (1996).
- ¹³M. Duraj, R. Duraj, A. Szytula, and Z. Tomkowicz, *J. Magn. Mater.* **73**, 240 (1988).
- ¹⁴T. Mazet, G. Venturini, R. Welter, and B. Malaman, *J. Alloys Compd.* **264**, 71 (1998).
- ¹⁵Z.H. Cheng *et al.* (to be published).
- ¹⁶S. Radha, S.B. Roy, A.K. Nigam, and Girish Chandra, *Phys. Rev. B* **50**, 6866 (1994).
- ¹⁷J.H.V.J. Brabers, K. Bakker, H. Nakotte, and F.R. de Boer, *J. Alloys Compd.* **199**, L1 (1993).